Structure, Vol. 11, 253–263, March, 2003, ©2003 Elsevier Science Ltd. All rights reserved. PII S0969-2126(03)00027-3

Nucleotide-Induced Conformational Changes in an Isolated *Escherichia coli* DNA Polymerase III Clamp Loader Subunit

Marjetka Podobnik,[1,5] Tanya F. Weitze,[1] Mike O'Donnell,[4] and John Kuriyan[1,2,3,*]
[1]Department of Molecular and Cell Biology and
[2]Department of Chemistry
Howard Hughes Medical Institute
University of California, Berkeley
Berkeley, California 94720
[3]Physical Biosciences Division
Lawrence Berkeley National Laboratory
Berkeley, California 94720
[4]Howard Hughes Medical Institute
The Rockefeller University
1230 York Avenue
New York, New York 10021

Summary

Sliding clamps are loaded onto DNA by ATP-driven clamp loader complexes. The structure of the *E. coli* clamp loader in a nucleotide-free state has been determined previously. We now report crystal structures of a truncated form of the isolated γ-ATPase subunit, γ^{1-243}, of the *E. coli* clamp loader, in nucleotide-free and bound forms. The γ subunit adopts a defined conformation when empty, in which the nucleotide binding site is blocked. The binding of either ATPγS or ADP, which are shown to bind with equal affinity to γ^{1-243}, induces a change in the relative orientation of the two domains such that nucleotides can be accommodated. This change would break one of the γ:γ interfaces seen in the empty clamp loader complex, and may represent one step in the activation process.

Introduction

The remarkable speed of genomic DNA replication (approximately 750 nucleotides/s in *E. coli*) [1, 2] relies on the assistance provided to DNA polymerases by sliding clamps and their associated clamp loader assemblies (reviewed in [3, 4]). Sliding clamps are ring-shaped proteins [5, 6] whose role in replication is to provide a DNA-bound mobile platform to which the polymerase enzyme is tethered. Clamp loaders are DNA-dependent ATPase assemblies consisting of five subunits (reviewed in [3, 4]) that load sliding clamps onto DNA. In eubacteria, the sliding clamp (β subunit) is composed of two identical crescent-shaped protomers that assemble head-to-tail to form a ring [5]. The corresponding clamp loader complex contains three different subunits, γ, δ, and δ′, which form a minimal functional complex with the stoichiometry $\delta':\gamma_3:\delta$ [7–9], in which γ is an ATPase, δ′ is thought to be a stator, and δ is a "wrench" that opens the sliding clamp. DNA polymerase III holoenzyme contains two forms of the ATPase subunit, γ and τ. τ is a longer version of γ that is produced by a translational frameshift [10–13]. In terms of the clamp-loading function, γ and τ are interchangeable [14].

The crystal structure of the clamp loader assembly from *E. coli* has been determined recently in a nucleotide-free state [9]. The γ-ATPase, δ wrench, and δ′ stator subunits are related to each other structurally, and to the subunits of eukaryotic and archaeal clamp loader complexes known as replication factor C (RFC) [9, 15–18]. The clamp loader complex of T4 bacteriophage consists of two subunits (gp44 and gp62) [19], of which gp44 is related to the γ-ATPase subunit by sequence [17, 20]. The clamp loader subunits are related in structure to ATPases that constitute the large family of AAA+ ATPases [20].

The three kinds of subunits that form the clamp loader have distinct functions. The γ subunits bind ATP and power the action cycle of the clamp loader [13, 21]. The δ subunit wrench has high affinity for the β clamp, and is the one subunit in the clamp loader that can open the β clamp on its own [22, 23]. The δ′ subunit is thought to be a stator that bridges the γ and δ subunits and somehow prevents interactions between the δ wrench and the β clamp when the complex is not active [9, 17, 23, 24]. The clamp loader complex undergoes substantial but as yet undefined conformational changes upon ATP binding. These conformational changes are thought to release the δ wrench so that it can interact with the β clamp [22, 25].

Each clamp loader subunit is composed of three domains (I, II, and III). The region of similarity to AAA+ ATPases spans the first two domains of each subunit, which together constitute the nucleotide binding segment of the subunit [18, 23, 26, 27]. The C-terminal helical domains (III) of each subunit associate to form a circular collar, from which the N-terminal domains are suspended [9].

As in other AAA+ ATPases, the ATP binding sites are located at the interfaces between subunits (Figure 1A) [18, 23, 26, 27]. The structural response to nucleotide binding, hydrolysis, and release is still poorly understood for the clamp loaders. Domains I and II contain two conserved sequence motifs that were inferred to be sensors that respond to the nucleotide (Figure 1B) [17]. Sensor 1 is located in domain I and corresponds to the "switch 2" region of G proteins such as Ras [28, 29]. The clamp loader subunits have no element corresponding to the "switch 1" element in Ras. Instead, structural analogy to adenylate kinase [30], coupled with sequence conservation and mutational data, identified a second sensor region (sensor 2), in domain II [17, 26, 27, 31]. The sequence motifs that comprise these two sensors are conserved in clamp loaders from bacteria, archaea, T4 bacteriophage, and eukaryotes [17].

Although each of the γ-ATPase subunits in the crystal structure of the clamp loader complex [9] is in the same

*Correspondence: kuriyan@uclink.berkeley.edu
[5]On leave from the Department of Biochemistry and Molecular Biology, Jozef Stefan Institute, Ljubljana, Slovenia.

Key words: AAA+ ATPase; clamp loader; DNA polymerase III; γ subunit; replication factor C (RFC)

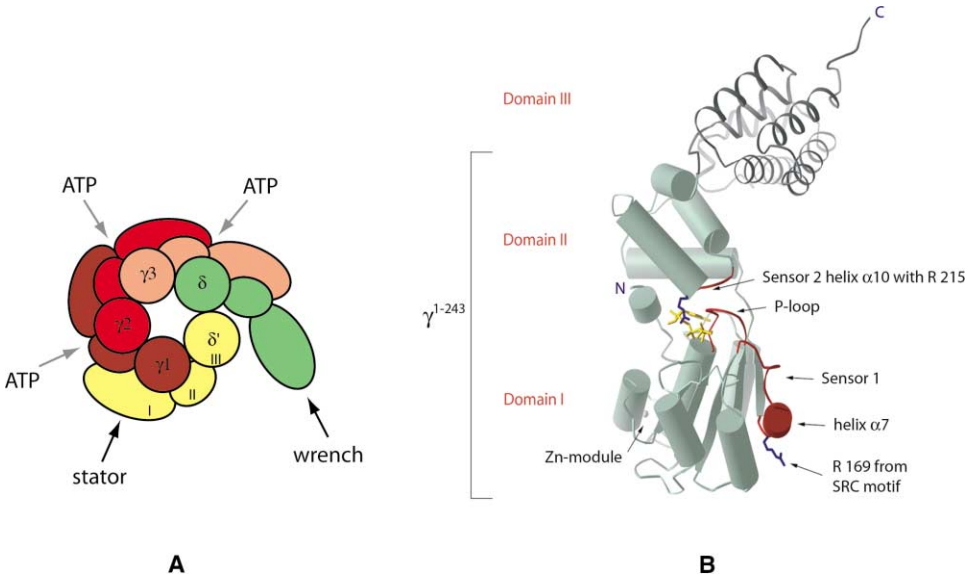

Figure 1. *E. coli* Clamp Loader Assembly and Structure of the γ-ATPase Subunit

(A) Schematic diagram of the *E. coli* clamp loader complex in the nucleotide-free form, based on the crystal structure [9].

(B) Structure of the γ-ATPase subunit. For domains I and II, the structure shown is that of ATPγS complex (this work). The structure of domain III, responsible for oligomerization, is taken from the γ1 subunit of the intact clamp loader complex [9].

(B) and Figures 2, 4, and 5 were generated using Ribbons [51].

state with respect to bound nucleotide (i.e., empty), the structure is asymmetric. Each of the γ subunits has a unique conformation, with the differences between the subunits arising primarily from changes in the orientation of domain III with respect to domains I and II. The interfaces between each of the subunits are strikingly different. In particular, considering just the two interfaces between the three γ-ATPase subunits, one of these (γ1-γ2) is tightly sealed and the other (γ2-γ3) is wide open. A proposed mechanism for clamp loading involves conversion, by ATP, of the clamp loader from a state in which both γ-γ interfaces are sealed shut, to one in which both are open and the δ subunit is released [9]. Biochemical data suggest that a subsequent step in the mechanism involves the DNA-induced hydrolysis of ATP and the resetting of the clamp loader [21, 32, 33], but how this happens is not understood.

In this paper, we address two questions regarding nucleotide binding that were raised by the structure of the *E. coli* clamp loader complex. First, in each of the empty γ-ATPase subunits, the sensor 2 region (helix α10) in domain II occludes the ATP binding site. Nucleotide binding must induce relocation of helix α10, but the nature of this conformational change and its consequences for the clamp-loading mechanism remain to be understood. Another question concerns the relationship between nucleotide binding and the tight packing between two of the γ-ATPase subunits (γ1 and γ2). The nucleotide binding site of γ2 is sealed shut by an α helix (α7) of the γ1 subunit that directly follows the sensor 1 (switch 2) region of γ1. This raised the question as to whether nucleotide binding to γ1 triggers a localized and internal conformational change in the sensor1/switch 2 region, such as in Ras, that results in the removal of helix α7 from the nucleotide binding site of γ2.

Insights into how nucleotides bind to clamp loader subunits have been provided by the structure of the small subunit (RFCS) of archaeal RFC, which has been visualized in both empty and ADP-bound states [18]. The sequence identity between RFCS and the γ subunit is relatively low (35% in domains I and II). The organization of bacterial clamp loaders, which form heteropentamers of three distinct subunits, is also different from that of archaeal clamp loaders, which contain only two kinds of subunits (reviewed in [3, 4]). These factors make it difficult to draw precise connections between the mechanisms of the *E. coli* and archaeal clamp loaders at this stage.

Attempts to produce crystals of the intact *E. coli* clamp loader assembly bound to nucleotides have not as yet been successful. As a first step toward understanding the consequences of nucleotide binding to the γ-ATPase subunit of the *E. coli* clamp loader, we have designed and produced a truncated version of the γ-ATPase subunit containing only the nucleotide binding domains I and II (γ^{1-243}). γ^{1-243} lacks the C-terminal domain (domain III) responsible for oligomerization and is therefore monomeric in solution. We now describe the structural changes that occur within the isolated γ-ATPase subunit upon binding nucleotides, and report the results of calorimetric measurements of the binding affinities of ADP and ATP for γ^{1-243}.

Results and Discussion

Structure Determination

γ^{1-243}, comprising domains I and II of the *E. coli* γ subunit, was expressed in *E. coli* with an N-terminal glutathione S-transferase (GST) tag. The GST tag was removed proteolytically before crystallization (see Experimental Pro-

Table 1. Data Collection and Refinement Statistics

A. γ^{1-243} Nucleotide Crystals (Data to 2.3 Å)—MAD Phasing

Data Set	No. of Reflections (Total/Unique)	Completeness (%)	R_{sym}
$\lambda 1 = 1.28201$ Å	1,061,344/45,447	96.5 (84.4)	5.3 (24.0)
$\lambda 2 = 1.28243$ Å	1,071,022/45,684	96.2 (82.8)	5.8 (38.9)
$\lambda 3 = 1.24345$ Å	1,081,174/45,822	95.8 (83.4)	6.9 (49.8)
Mean overall figure of merit (15.0–2.3 Å) (centric/acentric) = 0.27/0.27			

Nucleotide-Free γ^{1-243} Crystals (Data to 2.2 Å)

Data Set	No. of Reflections (Total/Unique)	Completeness (%)	R_{sym}
$\lambda = 1.000$ Å	255,606/23,273	92.1 (79.0)	4.0 (33.8)

B. Refinement and Stereochemical Statistics

Crystal	γ^{1-243} Nucleotide	Nucleotide-Free γ^{1-243}
R value (%)	21.1	23.5
Free R value (%)	25.0	26.5
Average B factors[a] (Å^2)		
Main chains	31.7	45.8
Side chains and waters	34.7	49.3
Whole	33.1	47.4
Nucleotide[b]	24.2 (A), 33.2 (B), 26.7 (C), 29.1 (D)	
Rms deviations		
Bonds (Å)	0.0074	0.0082
Angles (°)	1.347	1.477

$R_{sym} = 100 \times \Sigma|I - <I>|/\Sigma I$, where I is the integrated intensity of a given reflection. For R_{sym} and completeness, numbers in parentheses refer to data in the highest resolution shell.
Figure of merit $= < |\Sigma P(\alpha) e^{i\alpha}/\Sigma P(\alpha)| >$, where α is the phase and $P(\alpha)$ is the phase probability distribution.
R value $= 100 \times \Sigma|F_p - F_p(calc)|/\Sigma F_p$, where F_p is the structure factor amplitude. The free R value is the R value for a 10% subset of the data that was not included in the crystallographic refinement.
[a] Average B factors for the molecules in the asymmetric unit.
[b] Average B factors for the nucleotides in molecules A, B, C, and D.

cedures). γ^{1-243} was crystallized in the presence of $MgCl_2$ and the ATP analogs ATPγS or AMP-PNP. Crystallization of γ^{1-243} was also attempted in the presence of ADP, but failed.

The structure of γ^{1-243} was first determined by molecular replacement using X-ray data measured from crystals grown in the presence of AMP-PNP. The analysis revealed no electron density for the nucleotide in the structure. This could be due to the low binding affinity of this nucleotide (AMP-PNP does not support the clamp-loading reaction [34] and binds less tightly to γ^{1-243} than does ATPγS; see below) as well as to the presence of sulfate ions in the crystallization conditions [0.12 M–0.19 M $(NH_4)_2SO_4$], which might have displaced the nucleotide. The resulting structure was refined to 2.2 Å resolution (Table 1), and provides a reference for the empty (nucleotide-free) form of γ^{1-243}.

In the presence of ATPγS, γ^{1-243} formed orthorhombic crystals of space group $P2_12_12_1$, with four molecules (A, B, C, and D) per asymmetric unit. Molecular replacement using the structure of the γ subunit (domains I and II) from the clamp loader complex [9] was unsuccessful. Instead, phases were determined experimentally by multiwavelength anomalous diffraction (MAD) on a single crystal, using anomalous scattering from the endogenous zinc atom in the γ subunit (Figure 1B; Table 1). The four molecules in the asymmetric unit are organized into two pairs. The molecules within each pair (A:B and C:D) are related by 2-fold rotation axes and the two pairs are related to each other by a translation along the axis through the centers of both pairs. These noncrystallographic symmetry elements result in approximately the same molecular environment being generated around each of the four crystallographically independent nucleotide binding sites in the asymmetric unit.

At each nucleotide binding site, Arg-98 from a neighboring molecule is positioned so as to interact with the phosphate groups of ATPγS (not shown). This appears to disturb the magnesium binding site, and no magnesium ion is seen at any of the four sites. The relative positioning of these molecules does not appear to have physiological significance, because the inferred positions of the C-terminal domains bear no relationship to the architecture of the clamp loader complex [9].

Each of the four sites differs significantly in terms of electron density features corresponding to the nucleotide. Electron density for ATPγS is completely defined in the experimental electron density map at one site (molecule A; Figure 2). There is no density for the γ-phosphate for the nucleotide bound at molecule C and only weak density in molecules B and D. This could be due to slow hydrolysis of ATPγS in the course of the crystallization, with ADP trapped at certain sites in the crystal structure. None of the nucleotides has abnormally high temperature factors, suggesting that the nucleotide is fully bound at all the sites. The temperature factor for the phosphorus atom in the β-phosphate group ranges from 27 Å^2 (molecule C) to 36 Å^2 (molecule B). The corresponding values for the phosphorus atom of the γ-phosphate group are higher, ranging from 42 Å^2 in molecule

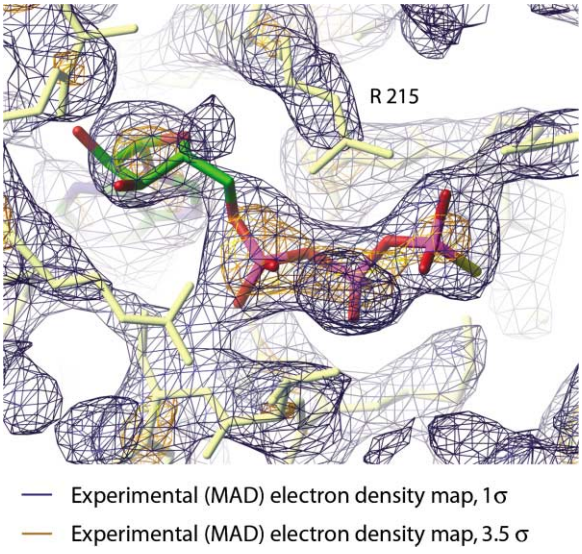

Figure 2. Experimental Electron Density Map (Density-Modified MAD Phases, Calculated to 3.0 Å Resolution) Showing the Position of ATPγS in Molecule A of γ^{1-243}

Dark blue and orange contour lines correspond to electron density at the 1 σ and 3.5 σ levels, respectively. Arg-215 from the sensor 2 region is indicated.

A to 62 Å^2 and 55 Å^2 in molecules B and D, respectively. Because there is no significant electron density for the γ-phosphate at site C, we assume that this corresponds to occupancy by ADP instead of ATPγS.

The two crystal structures we have determined provide us with views of three states of γ^{1-243}. A structure of empty γ^{1-243} is obtained in crystals grown in the presence of AMP-PNP. Crystals grown in the presence of ATPγS provide structures of the ATPγS complex (we shall use molecule A as a reference for this state) and of the ADP-bound form (for which we use molecule C as a reference).

The Nucleotide Binding Site

The structure of γ^{1-243} (Figure 1B) has all the elements that are typical of AAA+ ATPases, as seen before for the RFC subunit of an archaeal clamp loader [18]. The nucleotide is bound within a cleft at the interface between domains I and II (reviewed in [9, 18, 20, 35]). The adenine moiety of the nucleotide adopts an "anti" conformation with respect to the ribose, which retains the typical C3′-endo pucker. The adenine ring of the bound nucleotide is embedded in a hydrophobic environment and is sandwiched between Pro-12, part of the N-terminal helix α1, and Leu-214 in domain II.

In addition to these nonpolar contacts, the exocyclic amine (N6) of the adenine ring forms hydrogen bonds with the main chain carbonyl groups of Val-19 and Val-49, thus providing a means to distinguish between ATP and GTP. Both hydroxyl oxygens of the ribose, O2 and O3, are hydrogen bonded to the carbonyl oxygen of Ala-7 from the N-terminal helix α1. The phosphate groups of the nucleotide are coordinated by the residues of the conserved P loop (residues 41–52) [17]. Lys-51 forms a salt bridge to the β- and γ-phosphates (only to the β-phosphate in molecule C). Thr-52 and Ser-53 also form hydrogen bonds with the phosphate groups of the nucleotide.

Comparison of the structures of γ^{1-243} bound to nucleotides with that of the empty form reveals that the conformation of the closed state blocks the nucleotide binding site at the position of the ribose ring (Figure 3A). While the adenine ring and the phosphate groups fit into the "closed" binding pocket without major clashes with the protein, closure of the interdomain interfaces moves the sensor 2 region of domain II into a position that overlaps with the ribose group of ATP or ADP. Similar steric occlusion of the ribose binding site is also seen in all three γ subunits in the nucleotide-free clamp loader complex [9].

Nucleotide Binding Induces an Alteration of the Orientation of Domain I with Respect to Domain II

We have four views of the γ-ATPase subunit in an empty state, three from the clamp loader complex [9] and one from the present analysis (Figure 4). In each case, the γ subunit is in a very different environment with respect to interfacial interactions. Despite these differences, there is a striking conservation in the orientation of domain II with respect to domain I in each structure of an empty γ subunit. If the three γ subunits from the γ complex are superimposed on domain I of γ^{1-243}, the rms deviation in Cα positions in domain II ranges from 0.50 Å to 0.55 Å with respect to empty γ^{1-243}. The nucleotide binding site has collapsed in the structures of the empty γ-ATPase subunits, and has to expand in order to bind nucleotides.

The sensor 2 region (residues 212-GSLRDA-217) is located at the N terminus of helix α10 in domain II, and appears to play an important role in stabilizing an open, nucleotide-bound conformation of the domain (Figure 5). Nucleotide binding to γ^{1-243} results in a rotation of domain I with respect to domain II by 10°. Figures 4 and 5 show that binding of the nucleotide to the P loop in domain I is correlated with a movement of the sensor 2 region, which opens up the binding site. The side chain of Arg-215 blocks the nucleotide binding site in the nucleotide-free form, but swings away upon nucleotide binding and forms a salt bridge with the γ-phosphate ATPγS (Figure 5). A similar interaction is seen in the structure of the D1 domain of the AAA+ protein NSF, where Lys-708 from sensor 2 interacts with the phosphate groups of the nucleotide [26, 27]. However, in molecules B, C, and D of γ^{1-243}, Arg-215 does not interact with the phosphate groups of the nucleotide, resulting in less defined conformations and higher temperature factors (B) for the side chain of this residue, up to 15 Å^2 higher than for Arg-215 in molecule A (the side chain of Arg-215 in molecule A has an average B factor of ~30 Å^2). The well-defined conformation of Arg-215 in molecule A may be a result of having nucleotide triphosphate at high occupancy at this site.

The Sensor 1 (Switch 2) Region Does Not Change Conformation upon Nucleotide Binding

In Ras, the switch 2 region undergoes a large conformational change when GTP is hydrolyzed to GDP [29, 36].

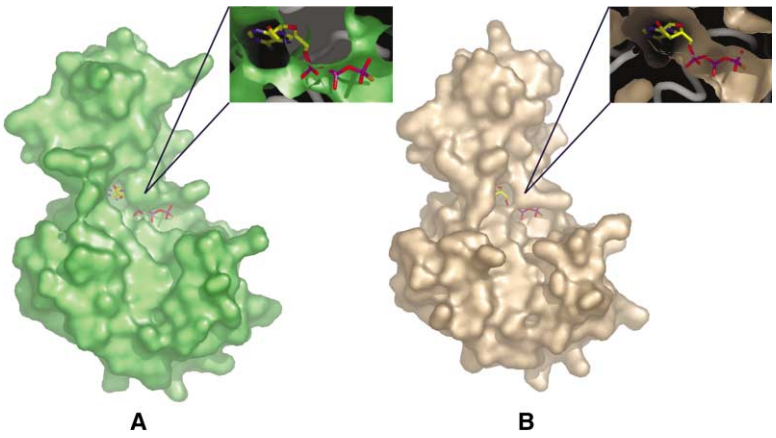

Figure 3. Changes at the Nucleotide Binding Site

(A) ATPγS from the structure of molecule A in the crystal structure of γ^{1-243} bound to nucleotides is superimposed onto the nucleotide binding site of the empty γ^{1-243} (green surface). The position of the nucleotide was defined by superimposing Cα atoms of the structure of ATPγS-bound γ^{1-243} onto domain I of empty γ^{1-243}.

(B) ATPγS in the ATPγS-bound γ^{1-243} (brown surface). The figure was generated using PyMOL [52].

By analogy to Ras, it was suggested that the sensor 1 region of clamp loader subunits might behave similarly [17]. In Ras, the γ-phosphate of GTP makes a hydrogen bond with the amide nitrogen of residue 60 in switch 2 [28, 29]. The presence of a glycine residue at position 60 in Ras enables the close interaction of the polypeptide backbone in the switch 2 region with the terminal phosphate of GTP, a feature that is crucial for the switching mechanism. Conformational changes in sensor 1 have been characterized for one AAA+ ATPase, the membrane-bound metalloprotease FtsH [37].

The sensor 1 region of the γ subunit includes the loop following strand β4 and helix α7 (residues 157–170; Figure 1B). Helix α7 contains a Ser-Arg-Cys (SRC) motif, which is conserved in clamp loader subunits in prokaryotes and eukaryotes [16, 38]. The arginine of the SRC motif is implicated in the interfacial stimulation of ATP hydrolysis [9], by comparison to the structures of hexameric AAA+ ATPases [26, 27, 39] and to the "arginine finger" provided by GTPase-activating proteins [20, 40].

The γ-ATPase subunit lacks a glycine residue in the corresponding region of sensor 1, which makes a close backbone interaction with ATP unlikely. Instead, the γ-ATPase subunit has a threonine residue (Thr-157) present in the corresponding position, and it was expected that a hydrogen bond would be formed between the side chain of Thr-157 and the terminal phosphate of ATP [17]. Indeed, in the structure of NSF-D2 [27], Ser-647 (corresponding to Thr-157 in γ) forms a hydrogen bond with the terminal phosphate of ATP. In structures of γ^{1-243} with bound ATPγS or ADP, Thr-157 is too far to make any contacts to the phosphates of the bound nucleotides, and the structure of the sensor 1 region in γ^{1-243} remains essentially unchanged upon nucleotide binding (not shown). If the ATPγS- and ADP-bound forms and the empty form of γ^{1-243} are superimposed using the central helix-turn-strand that comprises the P loop (residues 39–63), the rms deviation in all backbone atoms for the sensor 1 region (residues 157–170) is ~0.35 Å.

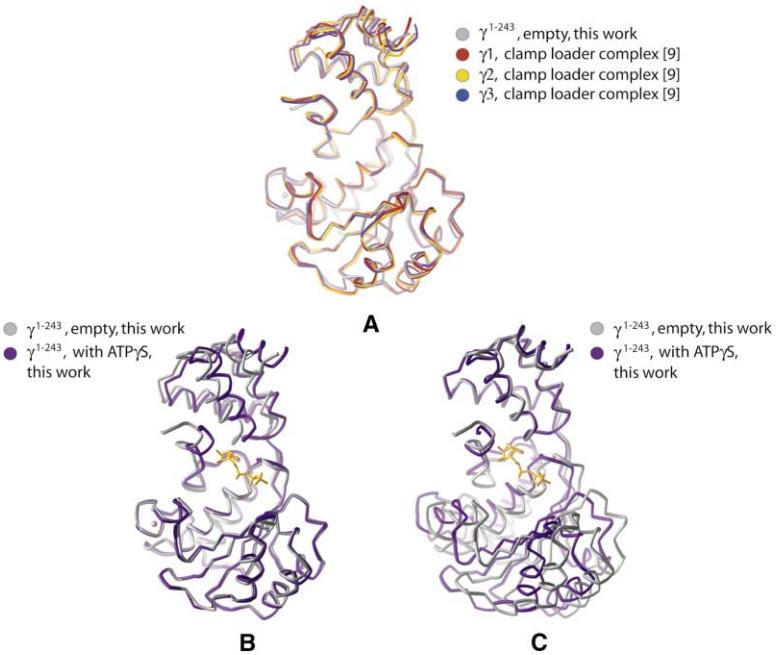

Figure 4. Changes in Domain I-Domain II Orientation

(A) Superposition of the nucleotide-free form of γ^{1-243} with the corresponding domains of the three γ subunits from the empty clamp loader complex [9]. The structures were superimposed using domain I only. Note the close correspondence in the orientation of domain II.

(B) Comparison of nucleotide (ATPγS)-bound and nucleotide-free forms of γ^{1-243}. The structures were superimposed on the residues of domain I.

(C) The molecules shown are the same as in (B), except that the superposition is on domain II.

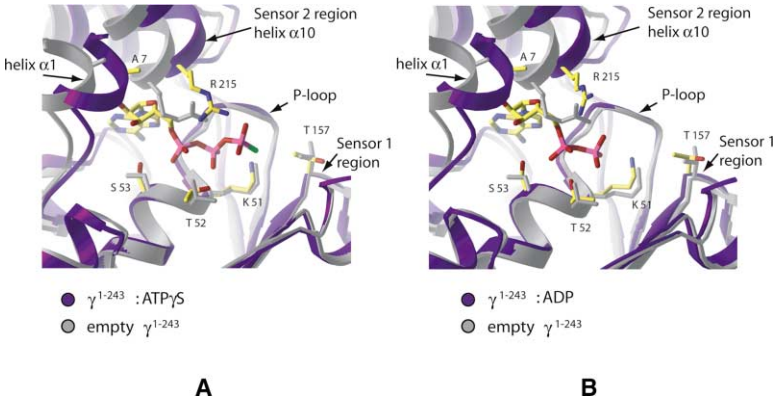

Figure 5. Comparison of the ATPγS- and ADP-Bound Forms of γ^{1-243}

(A) Nucleotide binding site in molecule A of the nucleotide complex of γ^{1-243} with bound ATPγS superimposed on domain I of the nucleotide-free form of γ^{1-243}. The side chains of some of the residues involved in binding the nucleotide are shown.

(B) Superposition of molecule C (ADP bound to γ^{1-243}) on the domain I residues of the nucleotide-free form of γ^{1-243}.

Comparison to the Small Subunit of Archaeal Clamp Loader (RFCS)

The RFCS subunit of archaeal clamp loader [18] has the same fold as the bacterial clamp loader subunits [9]. In crystals of RFCS from *Pyrococcus furiosus*, the protomers form two trimers [18]. Four of the six protomers in the crystal are bound to ADP, and the other two are empty. There is significant variability in conformations of the individual RFCS protomers, which do not show distinct differences that are characteristic of the presence or absence of ADP [18]. This is in contrast to our analysis of nucleotide binding to γ^{1-243}. As for *E. coli* γ^{1-243}, no major change in the sensor 1 conformation is observed when comparing the ADP-bound and free forms of the small subunits in RFC as well.

The nucleotide binding sites in the empty RFCS subunits do not seem to be as closed as in nucleotide-free γ^{1-243} (or γ subunits in the *E. coli* clamp loader [9]). There is also a significant difference in the relative orientations of domains I and II between RFCS and the γ-ATPase subunit. RFCS has an additional helix at the N terminus that is not present in the γ-ATPase subunit, and this helix makes close contacts to the sensor 2 helix in domain II of RFCS (corresponding to α10 in γ^{1-243}) [18]. The functional significance of these differences between the bacterial and archaeal clamp loader subunits is not clear at present.

Comparison to Protease-Associated ATPase HslU

One AAA+ ATPase system, the protease-associated ATPase HslU, has had its structure determined in the empty, ADP-bound, and ATP-bound states (reviewed in [41]). Interestingly, in this case, the primary consequence of nucleotide binding is a change in the orientation of domain II with respect to domain I, driven by the interactions between the sensor 2 region and the nucleotide. The magnitude of the conformational changes is similar to what we see with γ^{1-243}: domain II rotates with respect to domain I by approximately 10°–20°, but the details are different. In HslU, nucleotide binding induces a closure of the AAA+ module over the nucleotide. In γ^{1-243}, in contrast, nucleotide drives an opening of the AAA+ module. As in the γ^{1-243} structure, the region corresponding to sensor 1 does not undergo significant conformational changes upon nucleotide binding.

Binding Affinities of γ^{1-243} for Nucleotides

The close structural correspondence between the ATP- and ADP-bound forms of γ^{1-243} indicates that the isolated γ subunit may not differentiate significantly between ATP and ADP. To see whether this is the case, we used isothermal titration calorimetry (ITC) to measure the binding affinities of nucleotides for γ^{1-243}.

The analysis of nucleotide binding to the intact clamp loader assembly is complicated by the presence of multiple binding sites. The fact that γ^{1-243} lacks domain III, and therefore does not form oligomers, simplifies the analysis of calorimetric data. Initial experiments with the γ^{1-243} construct resulted in a stoichiometry of 0.5:1 (nucleotide:protein). The unexpectedly low stoichiometry appears to be due to a time-dependent change in the protein that affects nucleotide binding. Shortening the time spent during purification improved the apparent stoichiometry of binding. We therefore retained the GST tag and used freshly prepared GST-γ^{1-243}, rather than subject the protein to the overnight cleavage procedure that was used to remove the tag. The use of the GST fusion protein helped to improve the measured binding stoichiometry, with results close to 1:1, without affecting the binding affinity. The results of the ITC experiments (Figure 6) reveal that there is no significant difference between the affinities of ATPγS (K_d = 0.62 μM), ATP (K_d = 1.36 μM), and ADP (K_d = 1.03 μM) for γ^{1-243}, confirming that the isolated γ subunit cannot differentiate between ATP and its hydrolyzed form, ADP. The interaction of γ^{1-243} with AMP-PNP was also measured by ITC. The enthalpy change upon addition of AMP-PNP to γ^{1-243} was too low for accurate data fitting, and so K_d was not determined for AMP-PNP. Interestingly, AMP-PNP does not support the clamp loader-catalyzed clamp opening, while ATP and ATPγS are both effective to the same extent [25, 34].

Consequences for Clamp Loader Mechanism

Close similarity in the conformations of the ATP- and ADP-bound states of γ^{1-243} and the inability of γ^{1-243} to distinguish between ADP and ATP highlights the importance of interfacial interactions in the clamp loader mechanism. ATP, and not ADP, is required for the clamp loader to interact with the clamp [22]. Presumably, as yet uncharacterized interfacial interactions are responsible for this difference. Comparison with F_1-ATPase is in-

A

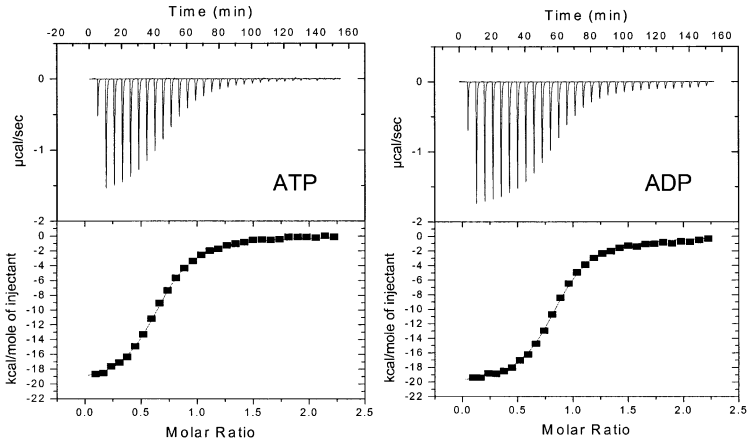

Figure 6. Isothermal Titration Calorimetry (ITC) Data for GST-Fused γ^{1-243} with Nucleotides

(A) Left: calorimetric titration for 300 μM ATP in the assay buffer injected into a 30 μM solution of GST-fused γ^{1-243}. Twenty-nine injections were performed. Right: calorimetric titration for 300 μM ADP in the assay buffer injected into a 30 μM solution of GST-fused γ^{1-243}. Titrations were also carried out for ATPγS and AMP-PNP (not shown).

(B) Values for K_d and binding enthalpy for each of the nucleotides used in ITC. n is the number of titrations carried out for each nucleotide and SD is the standard deviation. K_d for AMP-PNP was not determined due to the weak heat of binding observed.

B

Nucleotide	K_d (Mx10^{-6}) (SD)	ΔH(kcal/mol) (SD)
ATPγS (n=8)	0.62 (0.15)	-12.6 (2.7)
ATP (n=3)	1.36 (0.16)	-18.7 (0.6)
ADP (n=3)	1.03 (0.07)	-19.2 (3.7)

structive in this regard [42]. Both the ADP- and ATP-bound domains are structurally similar in that system, with interfacial interactions with the terminal phosphate of ATP being the distinguishing feature of the ATP-bound state [42].

There are three nucleotide binding sites in the *E. coli* clamp loader complex, located within γ1 (at the γ1-δ' interface), γ2 (at the γ2-γ1 interface), and γ3 (at the γ3-γ2 interface). In the structure of the empty clamp loader complex [9], the nucleotide binding site of γ2 is completely inaccessible, because the entire face of the domain is sealed shut by interactions with γ1. In contrast, the nucleotide binding sites of γ1 and γ3 are completely accessible. The consequences of nucleotide binding to γ3 are not readily apparent, as γ3 appears to be less constrained than γ1 and γ2, and could potentially adjust in various ways.

γ1 is interesting, however. Domains I and II of γ1 interact with γ2 and δ', respectively, in a way that is bound to change significantly upon nucleotide binding (Figure 7). Specifically, domain II of γ1 interacts with the SRC motif of δ'. This interaction involves helix α10 of γ1, which bears the sensor 2 region at its N terminus. The conserved arginine residue in the SRC motif of δ' is known to be important, because the mutation of this residue severely impairs ATPase activity and clamp loader function (A. Johnson and M.O.D., unpublished data). In the structure of the empty clamp loader [9], the SRC motif of δ' is wedged against domain II, and not the nucleotide binding site, of γ1. This interaction differs from that seen in the structures of hexameric AAA+ ATPases such as p97, where the corresponding arginine residue interacts with the phosphate groups of nucleotide bound at the interfacial binding site [39]. We expect that such an interfacial alignment will indeed occur at some stage of the reaction cycle of the clamp loader, and that the observed γ1-δ' interactions will have to be broken for that to occur.

The other bridging interactions that γ1 makes is with γ2. Here, γ1 is positioned so that its SRC motif is wedged into the nucleotide binding face of γ2, but in a nonproductive manner. Figure 8 illustrates the fact that the nucleotide-bound conformation of γ^{1-243} is such that it cannot interact simultaneously with both γ2 and δ' in the manner seen in the structure of the empty complex. We therefore speculate that γ1 will be released from γ2 upon nucleotide binding, which might further lead to interactions between δ' and nucleotide bound to γ1, through the SRC motif of δ'. This concept is illustrated schematically in Figure 8.

Biological Implications

Our analysis of γ^{1-243} has revealed a systematic conformational difference between the empty and nucleotide-bound forms of the γ subunit. This involves a change in the relative orientation between domains I and II, which results in an opening of the nucleotide binding site and a change in the shape of the γ subunit that appears sufficient to rupture the tight interaction between two of the γ subunits in the empty complex. Our studies with the isolated γ subunit show that both ATP and ADP are

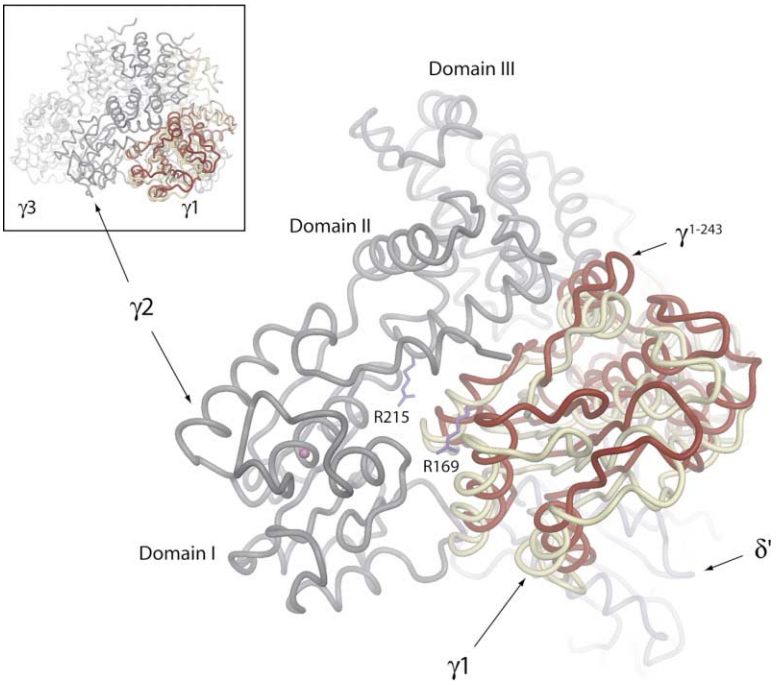

Figure 7. Potential Conformational Change at the γ1-γ2 Interface Induced by Nucleotide Binding

The structures of γ1, γ2, and δ′ from the empty clamp loader complex [9] are shown (γ1: light yellow; γ2, δ′: gray). ATPγS:γ^{1-243} (red) was superimposed onto domain II of γ1, suggesting that the tight γ1-γ2 interface must break apart upon nucleotide binding to γ1. Arg-215 from γ2 sensor 2 region and Arg-169 from γ1 SRC motif are shown in blue. Zinc atoms are shown as magenta spheres. The figure was generated using DINO [53].

able to induce similar transitions from a closed to an open form of the ATPase subunit. The ability of ATP, but not ADP, to drive clamp loading must therefore arise from interfacial interactions in the assembled clamp loader that distinguish between the subunits. Further experiments including all the subunits of the clamp loader complex are needed to fully characterize the sequence of events upon the binding of the nucleotides at the subunit interfaces, to understand the role of conformational changes and the residues at those interfaces in the process of loading the sliding clamps onto DNA.

Experimental Procedures

Preparation of the γ^{1-243} Construct

A cDNA fragment corresponding to residues 1–243 (domains I and II) of *E. coli* γ subunit (GenBank accession number X04487) was amplified by polymerase chain reaction and cloned into the pGEX vector (Amersham Biosciences). The construct referred to as γ^{1-243} contains a 5′ extension that includes the gene for glutathione S-transferase (GST), followed by the cleavage sequence for tobacco etch virus (TEV) protease. The GST-γ^{1-243} fusion protein was overexpressed in BL21-DE3 cells at 20°C overnight after induction with IPTG. Harvested cells were kept at −80°C.

The thawed cell mass was resuspended in 50 mM Tris/HCl (pH 8.0), 200 mM NaCl, 10% glycerol, 2 mM DTT, lysed in a French press (Avestin), and centrifuged. Clarified extract was loaded onto a glutathione Sepharose Fast Flow column (Amersham Biosciences). The bound protein was eluted with 20 mM glutathione (reduced form; Sigma) dissolved in the lysis buffer. The eluted protein was dialyzed against 50 mM HEPES (pH 7.0), 50 mM NaCl, 5% glycerol, 2 mM DTT. TEV protease was added to the dialyzed protein and the cleavage was carried out at 15°C for 40 hr. The purification was continued by a second passage through the glutathione Sepharose column in 50 mM HEPES (pH 7.0), 50 mM NaCl, 5% glycerol, 2 mM DTT. TEV protease was removed by flowing the sample over a Hi-

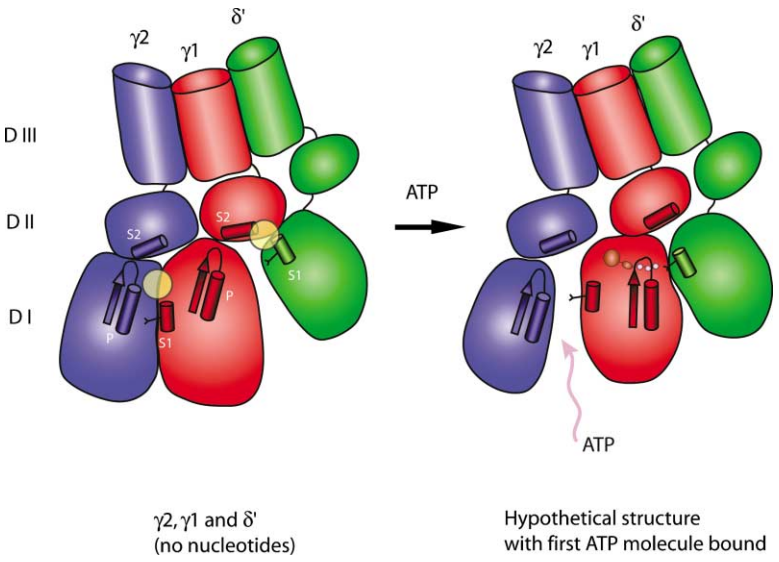

Figure 8. Schematic Diagram of Potential Rearrangement in the Clamp Loader Complex upon Nucleotide Binding

This represents a hypothetical sequence of events based on structural and biochemical evidence of conformational changes presented here and in [9]. Only three subunits of the γ complex are shown for clarity. Green: δ′; red: γ1; blue: γ2. S1: sensor 1/switch 2 helix α7, containing the SRC motif; P: P loop; S2: sensor 2 helix α10. Close contacts between the subunits are marked by yellow circles. ATP is drawn bound to the γ1 subunit (brown circles are for the base and sugar, and white are for the phosphate groups). Arginine from the conserved SRC motif is indicated on the S1 (sensor 1) helices.

Trap SP Sepharose HP column (Amersham Biosciences) equilibrated in the same buffer as the second glutathione Sepharose column. The flowthrough was dialyzed against 50 mM Tris/HCl (pH 8.5), 50 mM NaCl, 5% glycerol, 2 mM DTT and applied onto an ion exchange Source Q column. The protein was eluted by a linear gradient of NaCl, up to 350 mM. The final purification step included gel filtration on Superdex S-75 (Amersham Biosciences) in 20 mM Tris/HCl (pH 8.0), 50 mM NaCl, 2 mM DTT. The pure protein was concentrated to ~30 mg/ml. The identity of the sample was checked by N-terminal sequencing and mass spectroscopy. The recombinant protein contains an additional 7 residues at its N-terminal end (with the sequence GAHMGGS) that remain attached to the protein after cleavage of the GST tag.

For the GST-fused γ^{1-243} used in the ITC experiments, the protein eluted from the first glutathione Sepharose Fast Flow column was flown over a HiPrep desalting column (Amersham Biosciences), and the protein was frozen as GST fusion at −80°C.

Crystallization, Data Collection, and Processing

ATPγS and $MgCl_2$ were added to 1 mM γ^{1-243} to a final concentration of 5.0 mM and 12 mM, respectively. Crystals of the nucleotide-bound protein grew in 15% PEG 10K, 0.1 M KNO_3, 4% 1,4-butanediol. Crystals were cryoprotected with 25% glycerol added to the basic crystallization conditions.

The crystals of nucleotide-free γ^{1-243} grew from samples that contained AMP-PNP and $MgCl_2$ (1 mM protein, 12 mM AMP-PNP, 27 mM $MgCl_2$). The protein crystallized in the presence of 12%–19% PEG 3350, 0.12–0.19 M $(NH_4)_2SO_4$. The crystals were protected with 25% glycerol. AMP-PNP did not cocrystallize with the protein, and the structure was treated as that of the nucleotide-free form of γ^{1-243}.

Crystals of γ^{1-243}:ATPγS diffracted X-rays beyond 2.3 Å at beamline 5.0.2 (Advanced Light Source, ALS, Berkeley). They belong to space group $P2_12_12_1$, with cell constants a = 71.7 Å, b = 113.3 Å, c = 121.3 Å, with four molecules per asymmetric unit and 46% solvent content. The endogenous zinc atom from the Zn binding module in domain I of γ^{1-243} (one zinc atom per molecule) was used as a source of anomalous signal in a three-wavelength MAD experiment (Table 1). All data were integrated and reduced with DENZO/SCALEPACK [43]. The scaled and reduced intensity data were converted to amplitudes using TRUNCATE [44], and crosswavelength scaling was performed using FHSCALE [44], treating λ2 as native (Table 1). The positions of the four zinc sites in the asymmetric unit were determined using SOLVE [45]. Phase calculation and heavy atom refinement were performed in MLPHARE [44], and map modifications were carried out using DM [44] and MAMA [46]. Automated solvent flattening resulted in an electron density map of high quality into which a model for the γ^{1-243} was fitted using the program O [47].

Crystals of γ^{1-243} grown in the presence of AMP-PNP diffracted X-rays beyond 2.2 Å at beamline 8.3.1 (ALS, Berkeley; Table 1). These crystals belong to space group $P2_1$, with cell constants a = 47.3 Å, b = 85.5 Å, c = 56.9 Å; β = 93.2°, with 41% solvent content and two molecules per asymmetric unit. The positions of the molecules were found using molecular replacement (AMoRe) [48], using the first two domains of the γ2 subunit [9] as a search model. Initial electron density maps indicated that the nucleotide binding site was empty and that the site was blocked by the relative orientation of domains I and II.

Models for both structures were built using O [47] and refined using CNS [49] (Table 1). For the ATPγS-bound structure, structure factors measured to 2.3 Å at λ1 were used for the refinement. The final model for the nucleotide-bound γ^{1-243} contains residues 5–243 and 364 water molecules. The final model for the nucleotide-free γ^{1-243} structure contains residues 4–243 and 162 water molecules, and a sulfate ion in the nucleotide binding site. All structures show weakly defined electron density in the region of residues 99–110 (helix α5) as well as for the first 5 N-terminal residues and residue number 243. The geometry was analyzed using PROCHECK [50]. In the nucleotide-bound form, 91.4% of the residues are in the most favored regions of the Ramachandran plot, and no residues are in the disallowed regions. In the nucleotide-free structure, 88.1% of the residues are in the most favored regions and no residues are in the disallowed regions.

Isothermal Titration Calorimetry

ITC experiments were carried out using a MicroCal VP isothermal titration calorimeter (MicroCal). Proteins used in the experiments were the γ^{1-243} construct and the GST-fused γ^{1-243} (preparation described above). Calorimetric titrations were carried out using ATP, ATPγS, ADP, and AMP-PNP.

Solutions of nucleotides in water were adjusted to pH 7.0 with a minimum of NaOH and diluted into ITC buffer at a final concentration of 100 mM HEPES (pH 7.0), 50 mM NaCl, 5 mM $MgCl_2$ unless stated otherwise. Aliquots of γ^{1-243} were thawed, centrifuged at 4°C, and buffer exchanged using NAP™-5 desalting columns (Amersham Biosciences). Syringe and sample cell buffers contained the same final concentrations of all solutes. Concentration of γ^{1-243} before dilution into the final sample was measured by absorption at 280 nm with ϵ_{280} = 10810 M^{-1} cm^{-1} for γ^{1-243} and ϵ_{280} = 54530 M^{-1} cm^{-1} for γ^{1-243}-GST fusion.

After vacuum degassing samples, the nucleotide solution (150–300 μM) was titrated into protein solution (15–30 μM) in 10 μl injections, 300 s apart. Raw data for 29 injections at 25°C were obtained using the MicroCal VP-Viewer software. As a control, the nucleotides were titrated into the ITC buffer. There was no significant heat of dilution or injection for any of the tested nucleotides (not shown).

Raw ITC data were analyzed by integrating isotherms, subtracting baseline and background heat of injection, and fitting the parameters of the following equation for a one-site binding model with MicroCal Origin software.

$$Q = [(NM_t\Delta HV_0)/2][1 + X_t/NM_t + 1/NKM_t - ((1 + X_t/NM_t + 1/NK\,M_t)^2 - 4X_t/NM_t)^{1/2}]$$

$$\Delta Q(i) = Q(i) + (dV/V_0)[(Q(i) + Q(i-1))/2] - Q(i-1)$$

where K is the binding constant, N is the number of binding sites per protein molecule, V_0 is the active cell volume, M_t and [M] are the bulk and free concentration of macromolecule in V_0, respectively, X_t and [X] are the bulk and free concentration of nucleotide, respectively, and i is the injection number. The binding free energy and the entropy are derived using

$$\Delta G = -RT\ln K \text{ and } \Delta S = (\Delta H - \Delta G)/T$$

Acknowledgments

We thank David Jeruzalmi, Gregory D. Bowman, Holger Sondermann, and Bhushan Nagar for valuable assistance and discussions. We thank the staff at the 5.0.2 and 8.3.1 beamlines at the Advanced Light Source, Berkeley for assistance with synchrotron data collection. This work was supported by NIH grants GM45547 (J.K.) and GM38839 (M.O.D).

Received: October 17, 2002
Accepted: December 3, 2002

References

1. Stukenberg, P.T., Studwell-Vaughan, P.S., and O'Donnell, M. (1991). Mechanism of the sliding β-clamp of DNA polymerase III holoenzyme. J. Biol. Chem. *266*, 11328–11334.
2. Naktinis, V., Turner, J., and O'Donnell, M. (1996). A molecular switch in a replication machine defined by an internal competition for protein rings. Cell *84*, 137–145.
3. Ellison, V., and Stillman, B. (2001). Opening of the clamp: an intimate view of an ATP-driven biological machine. Cell *106*, 655–660.
4. O'Donnell, M., Jeruzalmi, D., and Kuriyan, J. (2001). Clamp loader structure predicts the architecture of DNA polymerase III holoenzyme and RFC. Curr. Biol. *11*, R935–R946.
5. Kong, X.P., Onrust, R., O'Donnell, M., and Kuriyan, J. (1992). Three-dimensional structure of the β subunit of *E. coli* DNA polymerase III holoenzyme: a sliding DNA clamp. Cell *69*, 425–437.
6. Krishna, T.S., Kong, X.P., Gary, S., Burgers, P.M., and Kuriyan,

J. (1994). Crystal structure of the eukaryotic DNA polymerase processivity factor PCNA. Cell *79*, 1233–1243.

7. Onrust, R., Finkelstein, J., Turner, J., Naktinis, V., and O'Donnell, M. (1995). Assembly of a chromosomal replication machine: two DNA polymerases, a clamp loader, and sliding clamps in one holoenzyme particle. III. Interface between two polymerases and the clamp loader. J. Biol. Chem. *270*, 13366–13377.
8. Pritchard, A.E., Dallmann, H.G., Glover, B.P., and McHenry, C.S. (2000). A novel assembly mechanism for the DNA polymerase III holoenzyme DnaX complex: association of δδ′ with DnaX(4) forms DnaX(3) δδ′. EMBO J. *19*, 6536–6545.
9. Jeruzalmi, D., O'Donnell, M., and Kuriyan, J. (2001). Crystal structure of the processivity clamp loader γ (γ) complex of *E. coli* DNA polymerase III. Cell *106*, 429–441.
10. Flower, A.M., and McHenry, C.S. (1986). The adjacent dnaZ and dnaX genes of *Escherichia coli* are contained within one continuous open reading frame. Nucleic Acids Res. *14*, 8091–8101.
11. Flower, A.M., and McHenry, C.S. (1990). The γ subunit of DNA polymerase III holoenzyme of *Escherichia coli* is produced by ribosomal frameshifting. Proc. Natl. Acad. Sci. USA *87*, 3713–3717.
12. Yin, K.C., Blinkowa, A., and Walker, J.R. (1986). Nucleotide sequence of the *Escherichia coli* replication gene dnaZX. Nucleic Acids Res. *14*, 6541–6549.
13. Tsuchihashi, Z., and Kornberg, A. (1990). Translational frameshifting generates the γ subunit of DNA polymerase III holoenzyme. Proc. Natl. Acad. Sci. USA *87*, 2516–2520.
14. Onrust, R., and O'Donnell, M. (1993). DNA polymerase III accessory proteins. II. Characterization of δ and δ′. J. Biol. Chem. *268*, 11766–11772.
15. Stillman, B. (1994). Smart machines at the DNA replication fork. Cell *78*, 725–728.
16. Cullmann, G., Fien, K., Kobayashi, R., and Stillman, B. (1995). Characterization of the five replication factor C genes of *Saccharomyces cerevisiae*. Mol. Cell. Biol. *15*, 4661–4671.
17. Guenther, B., Onrust, R., Sali, A., O'Donnell, M., and Kuriyan, J. (1997). Crystal structure of the δ′ subunit of the clamp-loader complex of *E. coli* DNA polymerase III. Cell *91*, 335–345.
18. Oyama, T., Ishino, Y., Cann, I.K., Ishino, S., and Morikawa, K. (2001). Atomic structure of the clamp loader small subunit from *Pyrococcus furiosus*. Mol. Cell *8*, 455–463.
19. Young, M.C., Reddy, M.K., and von Hippel, P.H. (1992). Structure and function of the bacteriophage T4 DNA polymerase holoenzyme. Biochemistry *31*, 8675–8690.
20. Neuwald, A.F., Aravind, L., Spouge, J.L., and Koonin, E.V. (1999). AAA+: a class of chaperone-like ATPases associated with the assembly, operation, and disassembly of protein complexes. Genome Res. *9*, 27–43.
21. Onrust, R., Stukenberg, P.T., and O'Donnell, M. (1991). Analysis of the ATPase subassembly which initiates processive DNA synthesis by DNA polymerase III holoenzyme. J. Biol. Chem. *266*, 21681–21686.
22. Naktinis, V., Onrust, R., Fang, L., and O'Donnell, M. (1995). Assembly of a chromosomal replication machine: two DNA polymerases, a clamp loader, and sliding clamps in one holoenzyme particle. II. Intermediate complex between the clamp loader and its clamp. J. Biol. Chem. *270*, 13358–13365.
23. Jeruzalmi, D., Yurieva, O., Zhao, Y., Young, M., Stewart, J., Hingorani, M., O'Donnell, M., and Kuriyan, J. (2001). Mechanism of processivity clamp opening by the δ subunit wrench of the clamp loader complex of *E. coli* DNA polymerase III. Cell *106*, 417–428.
24. Leu, F.P., Hingorani, M.M., Turner, J., and O'Donnell, M. (2000). The δ subunit of DNA polymerase III holoenzyme serves as a sliding clamp unloader in *Escherichia coli*. J. Biol. Chem. *275*, 34609–34618.
25. Hingorani, M.M., and O'Donnell, M. (1998). ATP binding to the *Escherichia coli* clamp loader powers opening of the ring-shaped clamp of DNA polymerase III holoenzyme. J. Biol. Chem. *273*, 24550–24563.
26. Lenzen, C.U., Steinmann, D., Whiteheart, S.W., and Weis, W.I. (1998). Crystal structure of the hexamerization domain of N-ethylmaleimide-sensitive fusion protein. Cell *94*, 525–536.
27. Yu, R.C., Hanson, P.I., Jahn, R., and Brunger, A.T. (1998). Structure of the ATP-dependent oligomerization domain of N-ethylmaleimide sensitive factor complexed with ATP. Nat. Struct. Biol. *5*, 803–811.
28. Brunger, A.T., Milburn, M.V., Tong, L., deVos, A.M., Jancarik, J., Yamaizumi, Z., Nishimura, S., Ohtsuka, E., and Kim, S.H. (1990). Crystal structure of an active form of RAS protein, a complex of a GTP analog and the HRAS p21 catalytic domain. Proc. Natl. Acad. Sci. USA *87*, 4849–4853.
29. Pai, E.F., Krengel, U., Petsko, G.A., Goody, R.S., Kabsch, W., and Wittinghofer, A. (1990). Refined crystal structure of the triphosphate conformation of H-ras p21 at 1.35 Å resolution: implications for the mechanism of GTP hydrolysis. EMBO J. *9*, 2351–2359.
30. Muller, C.W., and Schulz, G.E. (1992). Structure of the complex between adenylate kinase from *Escherichia coli* and the inhibitor Ap5A refined at 1.9 Å resolution. A model for a catalytic transition state. J. Mol. Biol. *224*, 159–177.
31. McAlear, M.A., Howell, E.A., Espenshade, K.K., and Holm, C. (1994). Proliferating cell nuclear antigen (pol30) mutations suppress cdc44 mutations and identify potential regions of interaction between the two encoded proteins. Mol. Cell. Biol. *14*, 4390–4397.
32. Hingorani, M.M., Bloom, L.B., Goodman, M.F., and O'Donnell, M. (1999). Division of labor—sequential ATP hydrolysis drives assembly of a DNA polymerase sliding clamp around DNA. EMBO J. *18*, 5131–5144.
33. Stewart, J., Hingorani, M.M., Kelman, Z., and O'Donnell, M. (2001). Mechanism of β clamp opening by the δ subunit of *Escherichia coli* DNA polymerase III holoenzyme. J. Biol. Chem. *276*, 19182–19189.
34. Turner, J., Hingorani, M.M., Kelman, Z., and O'Donnell, M. (1999). The internal workings of a DNA polymerase clamp-loading machine. EMBO J. *18*, 771–783.
35. Sousa, M.C., Trame, C.B., Tsuruta, H., Wilbanks, S.M., Reddy, V.S., and McKay, D.B. (2000). Crystal and solution structures of an HslUV protease-chaperone complex. Cell *103*, 633–643.
36. Milburn, M.V., Tong, L., deVos, A.M., Brunger, A., Yamaizumi, Z., Nishimura, S., and Kim, S.H. (1990). Molecular switch for signal transduction: structural differences between active and inactive forms of protooncogenic ras proteins. Science *247*, 939–945.
37. Niwa, H., Tsuchiya, D., Makyio, H., Yoshida, M., and Morikawa, K. (2002). Hexameric ring structure of the ATPase domain of the membrane-integrated metalloprotease FtsH from *Thermus thermophilus* HB8. Structure *10*, 1415–1423.
38. O'Donnell, M., Onrust, R., Dean, F.B., Chen, M., and Hurwitz, J. (1993). Homology in accessory proteins of replicative polymerases—*E. coli* to humans. Nucleic Acids Res. *21*, 1–3.
39. Zhang, X., Shaw, A., Bates, P.A., Newman, R.H., Gowen, B., Orlova, E., Gorman, M.A., Kondo, H., Dokurno, P., Lally, J., et al. (2000). Structure of the AAA ATPase p97. Mol. Cell *6*, 1473–1484.
40. Ahmadian, M.R., Stege, P., Scheffzek, K., and Wittinghofer, A. (1997). Confirmation of the arginine-finger hypothesis for the GAP-stimulated GTP-hydrolysis reaction of Ras. Nat. Struct. Biol. *4*, 686–689.
41. Wang, J., Song, J.J., Seong, I.S., Franklin, M.C., Kamtekar, S., Eom, S.H., and Chung, C.H. (2001). Nucleotide-dependent conformational changes in a protease-associated ATPase HslU. Structure *9*, 1107–1116.
42. Abrahams, J.P., Leslie, A.G., Lutter, R., and Walker, J.E. (1994). Structure at 2.8 Å resolution of F1-ATPase from bovine heart mitochondria. Nature *370*, 621–628.
43. Otwinowski, Z., and Minor, W. (1997). Processing of X-ray diffraction data collected in oscillation mode. Methods Enzymol. *276*, 307–326.
44. CCP4 (Collaborative Computational Project 4) (1994). The CCP4 suite: programs for protein crystallography. Acta Crystallogr. D *50*, 760–763.
45. Terwilliger, T.C., and Berendzen, J. (1999). Automated structure solution for MIR and MAD. Acta Crystallogr. D *55*, 849–861.
46. Kleywegt, G.J., and Read, R.J. (1997). Not your average density. Structure *5*, 1557–1569.
47. Jones, T.A., Zou, J.Y., Cowan, S.W., and Kjeldgaard, M. (1991).

Improved methods for binding protein models in electron density maps and the location of errors in these models. Acta Crystallogr. A *47*, 110–119.
48. Navaza, J. (1994). AMoRe: an automated package for molecular replacement. Acta Crystallogr. A *50*, 157–163.
49. Brunger, A.T., Adams, P.D., Clore, G.M., DeLano, W.L., Gros, P., Grosse-Kunstleve, R.W., Jiang, J.S., Kuszewski, J., Nilges, M., Pannu, N.S., et al. (1998). Crystallography & NMR system: a new software suite for macromolecular structure determination. Acta Crystallogr. D Biol. Crystallogr. *54*, 905–921.
50. Laskowski, R.A., MacArthur, M.W., Moss, D.S., and Thornton, J.M. (1993). PROCHECK: a program to check the stereochemical quality of protein structures. J. Appl. Crystallogr. *26*, 283–291.
51. Carson, M. (1997). Ribbons. In Methods in Enzymology, R.M. Sweet and C.W. Carter, eds. (New York: Academic Press), vol. 277, pp. 493–505.
52. DeLano, W.L. (2002). The PyMOL User's Manual (San Carlos, CA: DeLano Scientific), http://www.pymol.org.
53. Philippsen, A. (2002). Visualizing Structural Biology, http://www.dino3d.org.

Accession Numbers

Atomic coordinates of the free and nucleotide-bound forms have been deposited with the RCSB Protein Data Bank under ID codes 1NJG and 1NJF, respectively.